http://dx.doi.org/10.21577/0103-5053.20190168

J. Braz. Chem. Soc., Vol. 30, No. 12, 2567-2574, 2019
Printed in Brazil - ©2019 Sociedade Brasileira de Química

Article

Acid Hydrolysis of Regular Corn Starch under External Electric Field

Nádya P. da Silveira, *[a] *Roberta Zucatti,*[a] *Andrielle D. Vailatti*[a] *and Daiani C. Leite*[b]

[a]*Instituto de Química, Universidade Federal do Rio Grande do Sul, Av. Bento Gonçalves 9500, 90650-001 Porto Alegre-RS, Brazil*

[b]*Centro de Ciências Tecnológicas, Universidade do Estado de Santa Catarina, Paulo Malschitzki, 200, 89219-710 Joinville-SC, Brazil*

The main objective of the present work is the investigation of a new method for starch hydrolysis. For this, we proposed the acid hydrolysis under the action of an external electric field, able to develop a faster reaction than the conventional one. Corn starch with 18% amylose was subjected to a fixed voltage, varying the external electric field application time and the number of cycles. Morphology, crystallinity, and thermal stability of the starches were investigated by optical and scanning electron microscopy (SEM), X-ray diffraction (XRD), and small-angle X-ray scattering (SAXS). The results showed that the acid hydrolysis coupled with an external electric field allows a significant reduction in hydrolysis time, due to the orientation of the electrolyte ions. Cavities were observed at the surface of hydrolyzed starches after treatment. However, the principal feature is related to the increase of the granule crystallinity with increasing hydrolysis time. The results suggest that the starches treated by this new method are interesting candidates for application in the food industry if greater gelatinization resistance is required.

Keywords: acid hydrolysis, starch, electric field, crystallinity, SAXS

Introduction

Corn starch is an abundant biocompatible granular polysaccharide found in nature, extensively used in food industry,[1] adhesives,[2] pharmaceutical,[3] and waste treatment,[4] among others. Its semi-crystalline structure consists mainly of polymer chains of amylose and amylopectin associate by hydrogen bonds, forming a radial structural arrangement of crystalline and amorphous areas. The amylopectin chains are formed by α-D-glucopyranose connected by linear α-(1,4) and branched α-(1,6) links, whereas amylose chains are characterized by essentially linear structure of α-D-glucopyranose connected by α-(1,4) links.[5-8]

The internal organization of starch is due to its radial growth around a hilum (center of the granule). This characteristic can be observed through the ability of birefringence of the material with the exhibition under polarized light of what is known as Maltese cross.[8] The crystalline regions of the starch granule originate mainly from the amylopectin, specifically the linear parts of these branched chains, which are arranged in a double helical manner. The amylopectin branches and the amylose contribute to the amorphous fraction of the granules, the latter being located interposed to the crystalline regions, forming a lamellar structure.[8,9]

The lamellar structure provided by the periodicity of amorphous and crystalline regions found within the semi-crystalline shells, gives starch different physicochemical properties. The ability to chemically and/or physically modify the granules improves important characteristics for specific industrial applicability (such as size, porosity, thermal stability, mechanic resistance and amylose/amylopectin ratio, among others) and increases the search for easy and fast methodologies capable of causing such modifications.[10]

Generally the increase of crystallinity in starch granules is achieved by acid or enzymatic treatment[11] as a consequence of the primary hydrolysis of the amorphous regions, which have weaker intermolecular interactions and low degree of organization.[12] Acid hydrolysis, in particular, is considered one of the most common and cheap methods of modifying starch granules, because it is able to increase starch porosity and keep the granules intact.[13]

Depending on the purpose, the treatment via acid hydrolysis may last from few hours to several days.[14-17] Herein, we aimed the time optimization in order to produce

*e-mail: nadya@iq.ufrgs.br

modified starch granules with higher crystallinity and surface porosity without granule disruption. For that, our research proposes an acid hydrolysis of starch granules coupled with external electric field application.

Studies regarding the effect of pulsed electric field[18-21] and induced electric field[22,23] in starch granules are reported in the literature. However, the elevated applied electric fields lead to granule disruption and a consequent decrease in crystallinity.[23,24] The conditions applied in this work are related to the moderate electric field (MEF) method[24] with the electric field strength typically below 1000 V m^{-1}, which tends to be a non-thermal technique. The application of electric field during acid hydrolysis can orient ion migration into the granules and perform a more homogeneous and fast chemical effect, without granule disruption and increased crystallinity.

To the best of our knowledge, the achievement of the proposal described in this paper has not been reported in the literature yet and can contribute to better understand the MEF method.

Experimental

Materials

Regular corn starch (18% amylose) was a gift from Ingredion (Jundiaí, SP, Brazil) and it was dried at 40 °C for 48 h before use. Hydrochloric acid (HCl) (NEON, São Paulo, Brazil, 37%) and all other chemicals were of analytical or reagent grade and were used without purification.

Methods

Free acid hydrolysis (FAH)

A 5% (m/v) starch solution was prepared by dispersion of powder starch in 1.0 mol L^{-1} HCl and kept under hydrolysis for 24 h at room temperature (20 ± 3.0 °C). The sample was stirred once using a vortex stirrer (PHOENIX AP56, Brazil). After hydrolysis, the sample (FAH1) was centrifuged and washed several times with distilled water until neutral pH, then dried at 40 °C for 48 h. Finally, it was manually ground to powder in a porcelain grain.

Oriented acid hydrolysis (OAH)

Starch solutions (5% (m/v)) were prepared by dispersion of powder starch in 1.0 mol L^{-1} HCl, followed by electric field application (500 V m^{-1}) in a 2 V fixed voltage (adjustable power supply HF-3003S, Hikari, China). For this, a capacitor consisting of two semicircular gold electrodes parallel attached to a polytetrafluoroethylene (PTFE) support was used, as shown in Figure 1. The gold electrodes have a fixed separation of 4 mm and a quartz cuvette was used as sample holder. Different electric field application times and number of cycles were evaluated (Table 1). Purification steps were the same used in FAH preparation.

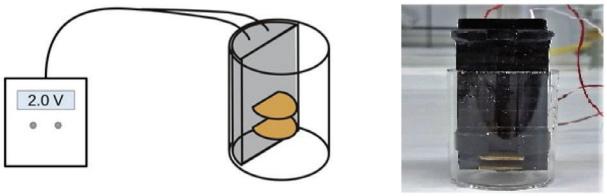

Figure 1. Experimental apparatus used for electric field application. Schematic representation (left) and real image (right).

Table 1. Electric field application times and number of cycles used in OAH

Sample	Number of cycles[a]	time of each cycle / s	Total time / s
FAH1	–	–	86.4×10^3
OAH1	1	10	10
OAH2	2	10	20
OAH3	5	10	50
OAH4	2	25	50
OAH5	3	20	60
OAH6	10	10	100

[a]Time interval between cycles (10 s). FAH: free acid hydrolysis; OAH: oriented acid hydrolysis.

Characterization

Scanning electron microscopy (SEM)

All samples were observed using an SEM instrument (EVO MA10, Zeiss, Germany). Samples were placed in stubs covered by a carbon tape and sputtered with an Au layer.

X-ray diffraction (XRD)

Analysis of regular corn starch and powder hydrolyzed samples were performed in a D-500 diffractometer (Siemens, Germany), operating at 40 kV and 17.5 mA from 3° to 40° 2θ. XRD patterns data were processed using OriginPro 2019 software[25] and smoothed with the Adjacent Averaging tool. Crystallinity degrees (X_C) were estimated by the method described by Hulleman *et al.*:[26]

$$X_C = \frac{H_C}{(H_C + H_A)} \quad (1)$$

where H_C is the intensity of the crystalline peaks and H_A is the intensity of the amorphous component of the peaks (background). Peaks centered in the region 15-30° 2θ were analyzed (see Figure 2).

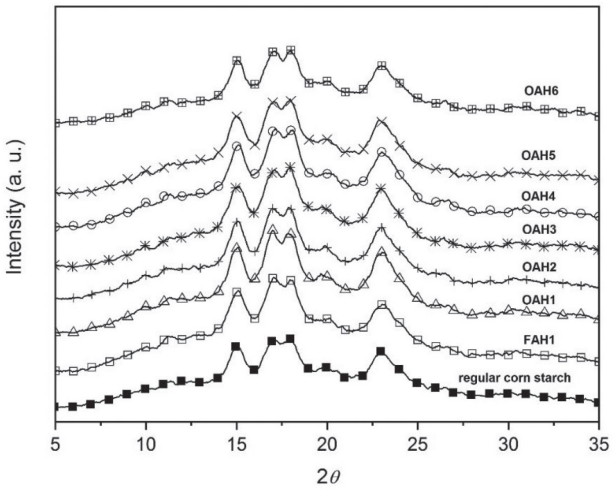

Figure 2. XRD patterns of starch samples.

Optical microscopy

Samples gelatinization temperature ranges were measured through optical microscopy under polarized light (BX41, Olympus, digital camera DP73, USA) with temperature control (oven FP82HT, Mettler Toledo and processor FP90, Mettler Toledo, USA). Samples were dispersed in distilled water (0.025 g mL^{-1}) and observed in a 10 °C min^{-1} heating hate, starting at 50 °C.

Small-angle X-ray scattering (SAXS)

The SAXS measurements of samples were performed on the D01B/SAXS1 beamline at the Laboratório Nacional de Luz Síncrotron (LNLS, Brazil). Starch pastes were prepared right before the measurement using dry treated starches and Milli-Q water (ratio 1:1) and the sample holder was sealed with adhesive tapes. The sample-to-detector distance was 3000 mm, covering a scattering vector q range of 0.04-1.5 nm^{-1}. Samples were kept at 20 ± 0.1 °C using a controlled thermobath. Water was measured as a background and subtracted from sample intensities, and it was also used for absolute normalization of the intensity. The exposure time in each sample was 10 min, and the wavelength of the incident radiation was 1.605 Å. SAXS data were fitted to a power law function (at small-q regime) according to equation 2 plus a Lorentzian peak (equation 3) or a Gaussian peak (equation 4) (at large-q regime),[27,28] using the non-linear fitting analysis in OriginPro 2019 software.[25]

$$I(q) = q^{-P} \quad (2)$$

$$I(q) = I_0 + \frac{2A}{\pi}\left(\frac{w}{4(q-q_0)^2 + w^2}\right) \quad (3)$$

$$I(q) = I_0 + \frac{Ae^{\frac{-4\ln(2)(q-q_0)^2}{w^2}}}{w\sqrt{\frac{\pi}{4\ln(2)}}} \quad (4)$$

where P is the power-law exponent, I(q) is the scattered intensity, I_0 is the background intensity, A is the peak area, w (nm^{-1}) is the full width at half maximum (FWHM) of the peak and q_0 (nm^{-1}) is the peak center position.

Results and Discussion

In acid hydrolysis, the hydronium ion attacks the oxygen in the glycosidic bond and later hydrolyses the linkage. Such attack primary occurs in amylose polymer chains linkages due to the better exposure of those hydrogen bonds in comparison with amylopectin polymer chains.[12] An acid works on the starch granule surface prior to entering the inner region of starch,[13] which means that the desirable effect in starch granules can be adjustable by the acid characteristics (such as ionic strength and concentration) and hydrolysis time, for example.[14,29-31] The acid hydrolysis coupled with external electric field application allows an oriented ion migration and a consequent hydrolysis time reduction. A simplified scheme of ion migration is shown in Figure 3. During free acid hydrolysis the ions diffusion is controlled by classical transport properties as ion concentration, ion size and temperature. Applying external electric field, the ionic diffusion becomes oriented and the hydronium ions attack is favored, increasing the linkage hydrolysis rate when compared with the classical acid hydrolysis method (FAH).

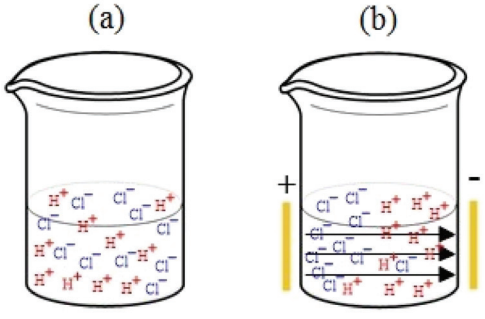

Figure 3. Simplified illustration of ionic diffusion in (a) free acid hydrolysis (FAH) and (b) oriented acid hydrolysis (OAH). The black arrows in (b) indicates the direction of the electric field.

The morphology of starch granules before and after the two acid hydrolysis methods proposed were observed using SEM (Figure 4). Regular corn starch granules present irregular shape with smooth surfaces (Figure 4a), as constantly reported in literature.[8,32]

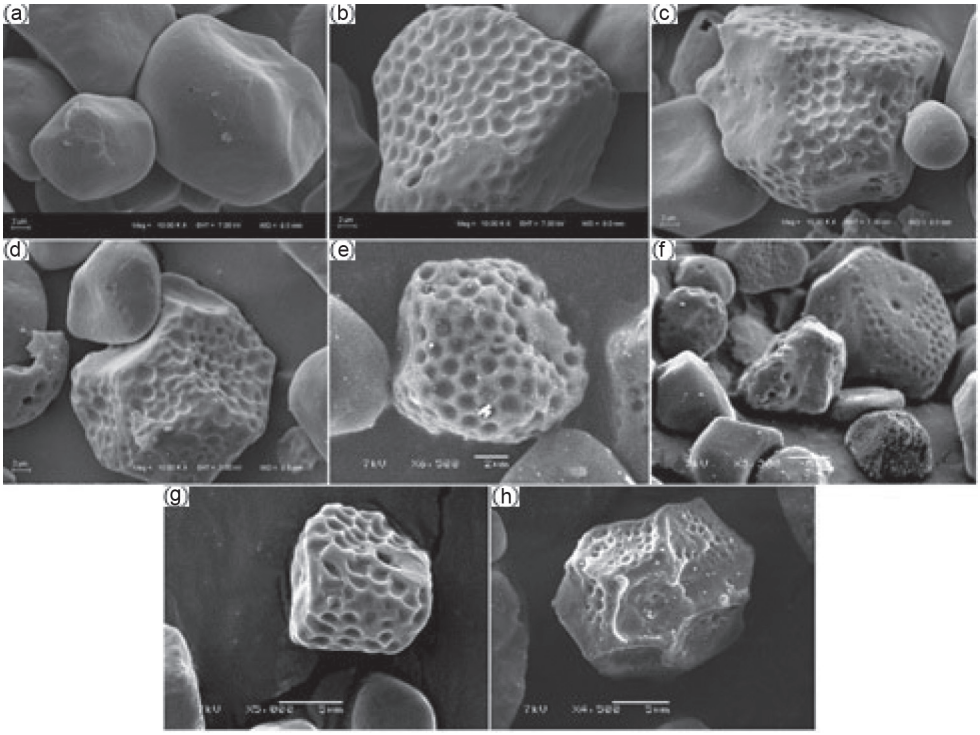

Figure 4. SEM images of (a) regular corn starch; (b) FAH1; (c) OAH1; (d) OAH2; (e) OAH3; (f) OAH4; (g) OAH5; and (h) OAH6.

As shown in Figures 4b-4h, acid modifications can alter physicochemical properties keeping regular the granule main structure. Some small cavities can be observed in all hydrolyzed starch granules due to the acid treatment. Similar surfaces were found either using FAH or OAH method, but the time optimization must be highlighted. To achieve the cavities on irregular surface of starch granules, sample FAH1 was submitted to 24 h of acid hydrolysis while all samples submitted to OAH presented similar effect in a much shorter time (see Table 1).

It is also noted that samples submitted to oriented acid hydrolysis possess subtle surface differences. According to the increase in number of cycles and time of each cycle the cavities in starch granule surface are more distinct and the entire surface is more irregular, with the polygonal shape pronounced.

Quantitative results regarding physicochemical properties of modified starches were achieved with XRD, optical microscopy and SAXS measurements. All starch samples presented a typical A-type crystalline structure profile, as can be seen in Figure 2.

Such profile is usually attributed to cereal species, with characteristic peaks at 15.0°, 17.0°, 18.0°, and 23.0° 2θ.[33,34] When starch granules are subjected to acid hydrolysis, the relative crystallinity increases with increasing hydrolysis time, as reported in Table 2.[17]

Table 2. Crystallinity degree and gelatinization temperatures of regular corn starch and hydrolyzed samples (FAH or OAH preparation method)

Sample	Number of cycles	time of each cycle / s	Total time / s	Crystallinity degree / %	Gelatinization temperature range[a] / °C	ΔT / °C
Regular corn starch	–	–	–	33.4	68.8-73.0	4.2
FAH1	–	–	86.4×10^3	39.7	56.8-69.5	12.7
OAH1	1	10	10	52.8	65.7-73.0	7.3
OAH2	2	10	20	49.3	68.0-74.0	6.8
OAH3	5	10	50	54.2	64.5-75.5	11.0
OAH4	2	25	50	51.4	65.0-75.0	10.0
OAH5	3	20	60	51.6	63.8-73.0	9.2
OAH6	10	10	100	48.6	64.4-69.5	5.1

[a]The first registered temperature is related to the beginning of Maltese cross disappearance, while the final registered temperature is related with the total Maltese cross disappearance. ΔT: gelatinization temperature range difference; FAH: free acid hydrolysis; OAH: oriented acid hydrolysis.

Among the most relevant physicochemical properties of starch is the gelatinization temperature, a phenomenon linked to the loss of structural organization due to the disruption of hydrogen bonds caused by the irreversible swelling of starch granules when heated in water.[35] This phenomenon occurs initially in the amorphous regions due to the fragility of hydrogen bonds in these areas, contrary to what happens in the crystalline regions.[5] Typically, high transition temperature ranges have been associated with high degrees of crystallinity, which provides structural stability and make the granules more resistant to gelatinization.[6] Table 2 shows the calculated crystallinity degree obtained from XRD patterns according to equation 1 and gelatinization temperature ranges obtained from optical microscopy.

It is quite well understood that acid hydrolysis increases the crystallinity degree of starch granules.[17,30,36,37] The crystallinity values for all OAH prepared samples are similar. Herein, we stand out the fast increase in crystallinity degree in such short times using OAH method. The crystallinity degree increased around 35% in OAH samples when compared to the regular corn starch. As can be seen in Table 2, samples prepared by OAH method presented higher crystallinity degree when compared to the sample prepared by FAH method for which the crystallinity increase was ca. 16%. The initial increase in relative crystallinity is due to a fast degradation of amorphous regions. After, when the central bulk amorphous regions and the amorphous growth rings are substantially degraded, there is little or no change in relative crystallinity due to the concomitant hydrolysis of crystalline and amorphous lamellae.[17]

The gelatinization characteristics of starches have been shown to be greatly influenced by the acid hydrolysis.[15,17,38] An increase in gelatinization temperature range takes place as a result of the increased crystallinity in acid hydrolyzed starches, as shown in Table 2. Other interpretations include that the preferential hydrolysis of amorphous regions attenuates the destabilizing effect of swelling in amorphous regions on the melting of the crystallites or that longer amylopectin double helices may form as a result of the removal of branch points.[17,39]

Analyzing the gelatinization onset and offset temperatures, it was observed that such ranges were narrower in OAH samples than in the FAH sample, indicating that the electric field application led to greater homogeneity during acid hydrolysis of the granules, since the gelatinization process (reflecting changes in crystallinity) was more evenly compared to the free hydrolysis. Another determining factor for the homogeneity of the oriented hydrolysis consisted of the number of electric field application cycles. The increase in the number of cycles (keeping the same total time) reduced the gelatinization range (samples OAH1 and OAH2), narrowing it even more than when only the total time of each cycle was increased (OAH4). Comparing samples OAH6 and OAH2 it is noted that the increase in the number of cycles maintaining the same total oriented hydrolysis time makes the range narrower too. If a relatively high crystallinity is desired together with a high gelatinization temperature range, then sample OAH3 proves to be the most appropriate. In this sample a larger number of cycles were applied, each in a shorter time when compared to the conditions of the other samples.

Small angle X-ray scattering has also been applied to study changes in the semi-crystalline structure of modified starch granules. All SAXS profiles were characterized by intense scattering at low q and a scattering peak at a characteristic q-value of 0.6-0.7 nm^{-1}, corresponding to the semi-crystalline lamellar structure of starch as related in the literature, as shown in Figure 5a.[40,41] Results of SAXS data fitting are reported in Table 3.

The scattering peak at q_0 is associated with the periodic arrangement of alternating crystalline plus amorphous regions inside the granule. Figure 5c brings in detail the mentioned peak for all samples. Samples prepared by OAH method present the same characteristic peak as observed for the regular corn starch, however, the intensity of the peak changes gradually according to the time and number of cycles of the electric field applied. It can be attributed mainly to the decrease in electron density of the amorphous growth rings as a result of preferential hydrolysis of these regions.[37]

The peak disappearance in the FAH1 sample is related to the loss of the internal organization structure of the granule. Regular corn starch and samples OAH1, OAH2, OAH3, and OAH4 could be fitted using a Lorentzian peak function, while sample OAH5 could only be fitted using a Gaussian peak function. The peak behavior observed in the sample OAH5 is related to a loosening of the intercalation between the amorphous and crystalline layers, although there is a maintenance of the crystallinity, tending to decrease when compared to the crystallinity observed in the sample OAH4, for example. The peak fit for sample OAH6 did not converge neither using a Lorentzian nor a Gaussian function probably due to the disordered structure obtained by conventional acid hydrolysis (24 h).

The widening of the SAXS peaks at q ca. 10 nm^{-1} in Figure 5, and the decrease of their relative intensity when compared to the regular corn starch indicates that lamellae composed of amylopectin, the main responsible for granule crystallinity, lose their long-range organization. It means

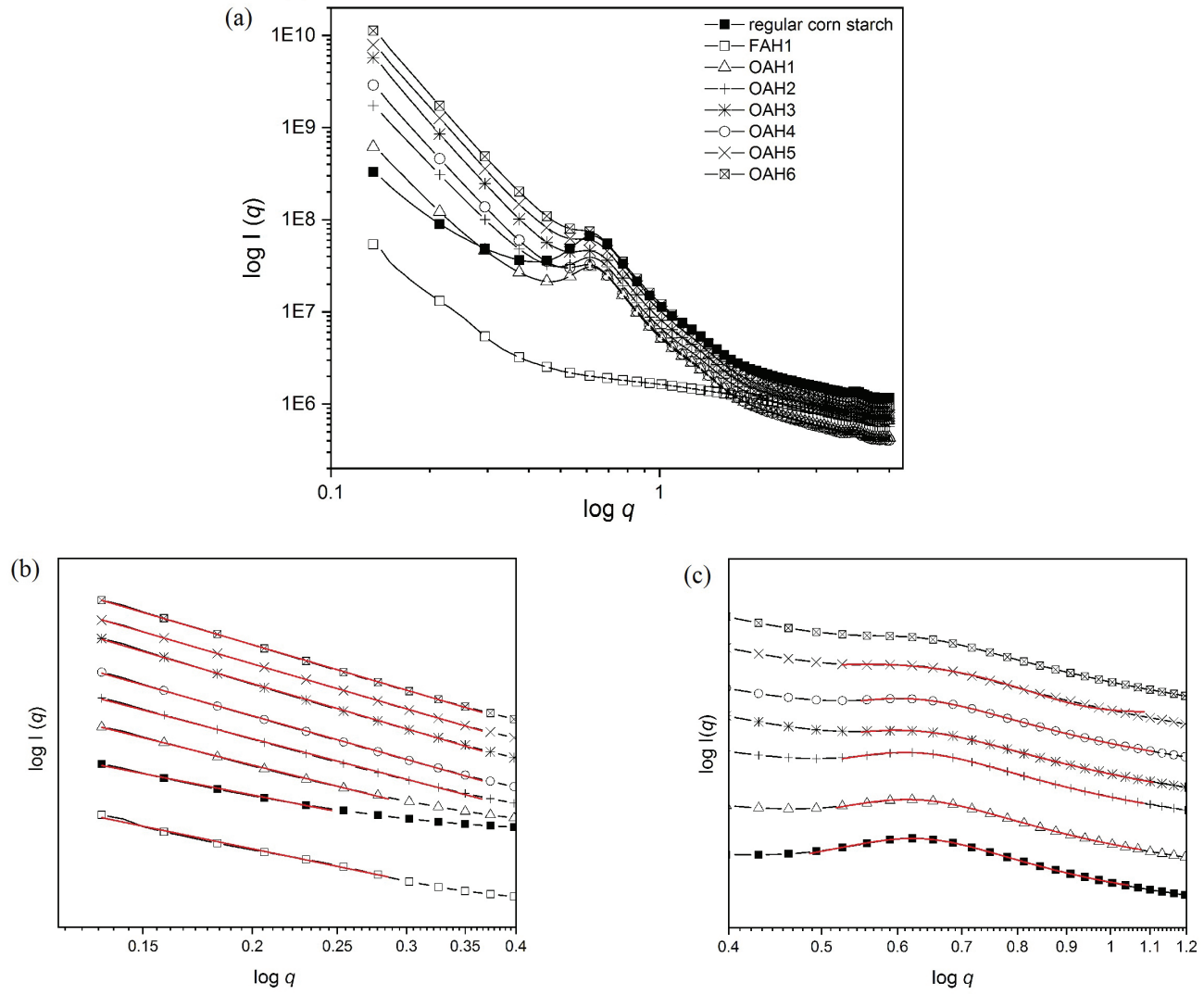

Figure 5. SAXS curves of samples covering all q-range measured (a); data fitting using a Power law model (b) and a Lorentz or a Gaussian function (c).

Table 3. SAXS data fitting, where q_0 is the peak center, L is the repeat distance ($2\pi/q_0$) and P is the power-law exponent

Sample	q_0 / nm^{-1}	L / nm	P
Regular corn starch	0.62	10.1	2.65
FAH1	no peak	–	2.80
OAH1	0.61	10.3	3.38
OAH2	0.61	10.3	3.55
OAH3	0.60	10.5	3.97
OAH4	0.60	10.5	3.82
OAH5	0.59	10.6	3.95
OAH6	0.59	10.6	3.99

FAH: free acid hydrolysis; OAH: oriented acid hydrolysis.

that the crystalline lamellae become more heterogeneous in thickness by the loss of small portions of amylose originally housed in these structures, but the nominal crystallinity (proved by XRD) tends to increase due to the increased packaging of the amylopectin chains during amylose outflow. Figure 6 shows the cross-section of an idealized starch granule, wherein the amylose and amylopectin layers succeed. After treatment the regions originally composed of amylose tend to decrease, giving rise to a predominance of amylopectin. However, the regions composed of amylopectin after treatment are no longer as homogeneous in thickness along the granule, as it can be seen along the dark pink rings that represent this macromolecule in Figure 6.

The repeat distance L tends to increase due to the relative growing of the lamellar distances during treatment, which influences the peak width and even the decrease in the relative height of the peak at q ca. 10 nm^{-1}. However, the peak is maintained for the different treatment conditions, with the exception of sample FAH1.

The power law exponent P in Table 3 is related to the characteristic surface of the granule. The regular corn starch

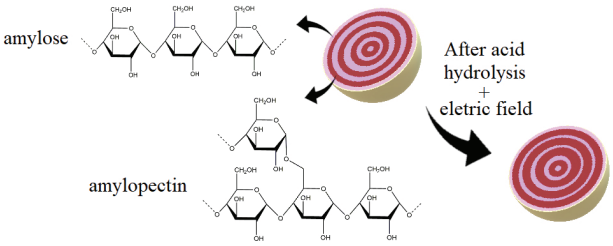

Figure 6. Cross-section of an idealized starch granule, wherein the starch main components are depicted as layers: amylose (light pink) and amylopectin (dark pink).

sample can be represented as a two-component system, with the granule distributed in the starch-water paste. The scattering signal fitted at low values of q (Figure 5b) is a Porod's law[42] resulting from the interface between water and the granules. After acid treatment the samples are altered and given origin to other Porod's law because small holes are created in each grain. The interface hole-granule changes the scattering law. A small value of P means a smooth surface whereas higher values can be attributed to the appearance of a surface roughness due to acid attack, as expected. Analysis of such spectra by means of a power law exponent can be applied to follow the progress of the granule surface attack during acid treatment. A comparison between the total time of treatment (Table 2) with the power-law exponent (Table 3) for each sample reveals a subtle but important difference; between 10 and 20 s of exposition the value of P is ca. 3.5 whereas for higher times, between 50 and 100 s of exposition the value of P becomes ca. 4.0. Indeed, the results shown in Figure 4 agree with this interpretation. For OAH1 and OAH2 samples the surfaces are more homogeneous with small recesses present, whereas for the OAH3-OAH6 samples a larger number of small holes may be observed, which are related to pores caused in the granules by the acid attack.

Conclusions

The results obtained by treatment of regular corn starch having 18% amylose indicate that the best reaction conditions are related to the application of an electric field with large number of cycles in a minimum time. The optimal reaction conditions for acid hydrolysis of regular corn starch under an electric field were 5 cycles of 10 s each. Under those conditions a relatively high crystallinity together with a high gelatinization temperature range of the treated starches are achieved. The new characteristics of the treated starch are mainly related to the loss of the amylose, the linear portion of the macromolecules in starch granule.

According to the increase in number of cycles and time of each cycle some of the cavities in starch granule surface become distinct and the entire surface seems to become more irregular as probed by scanning electron microscopy. The analysis by X-rays proved to be quite important for external and internal characterization of the modified starch granule. While X-ray diffraction indicated an enhancement of the crystallinity of the granules after treatment, small angle X-ray scattering revealed the surface fractality, ranging from 2.5 to 4.0. Regular starch and starch treated by conventional acid hydrolysis have the lowest values of fractality and after treatment the value tends to stabilize at 4.0 indicating a roughness surface due to acid attack, as expected.

The results suggest that starches treated by the new method are interesting candidates in food industry, since in a low amylose starch there will be less tendency for the retrograde phenomena during the cooling of the starch pastes.

Acknowledgments

The authors would like to thank CNPq (grant No. 405662/2016-5) for financial support and the Brazilian Synchrotron facility (LNLS/CNPEM, Proposal 20160060) for SAXS beam time. R. Z. and A. D. V. thank PROPESQ-UFRGS and CNPq for undergraduate fellowships.

References

1. Homayouni, A.; Amini, A.; Keshtiban, A. K.; Mortazavian, A. M.; Esazadeh, K.; Pourmoradian, S.; *Starch/Staerke* **2014**, *66*, 102.
2. Qiao, Z. B.; Gu, J. Y.; Lv, S. S.; Cao, J.; Tan, H. Y.; Zhang, Y. H.; *J. Adhes. Sci. Technol.* **2015**, *29*, 1368.
3. Scholtz, J.; Van der Colff, J.; Steenekamp, J.; Stieger, N.; Hamman, J.; *Curr. Drug Targets* **2014**, *15*, 486.
4. Ma, X. F.; Liu, X. Y.; Anderson, D. P.; Chang, P. R.; *Food Chem.* **2015**, *181*, 133.
5. Denardin, C. C.; Silva, L. P.; *Cienc. Rural* **2009**, *39*, 10.
6. Singh, N.; Singh, J.; Kaur, L.; Sodhi, N. S.; Gill, B. S.; *Food Chem.* **2003**, *81*, 219.
7. Buleon, A.; Colonna, P.; Planchot, V.; Ball, S.; *Int. J. Biol. Macromol.* **1998**, *23*, 85.
8. Perez, S.; Bertoft, E.; *Starch/Staerke* **2010**, *62*, 389.
9. Tester, R. F.; Karkalas, J.; Qi, X.; *J. Cereal Sci.* **2004**, *39*, 151.
10. Din, Z.-ud; Xiong, H.; Fei, P.; *Crit. Rev. Food Sci. Nutr.* **2017**, *57*, 2691.
11. Lacerda, L. D.; Leite, D. C.; Soares, R. M. D.; da Silveira, N. P.; *Starch/Staerke* **2018**, *70*, 1800008.
12. Angellier-Coussy, H.; Putaux, J. L.; Molina-Boisseau, S.; Dufresne, A.; Bertoft, E.; Perez, S.; *Carbohydr. Res.* **2009**, *344*, 1558.

13. Pratiwi, M.; Faridah, D. N.; Lioe, H. N.; *Starch/Staerke* **2018**, *70*, 1700028.
14. Angellier, H.; Choisnard, L.; Molina-Boisseau, S.; Ozil, P.; Dufresne, A.; *Biomacromolecules* **2004**, *5*, 1545.
15. Kim, H. Y.; Lee, J. H.; Kim, J. Y.; Lim, W. J.; Lim, S. T.; *Starch/Staerke* **2012**, *64*, 367.
16. Hu, X.; Wang, Y.; Liu, C.; Jin, Z.; Tian, Y.; *Starch/Staerke* **2018**, *70*, 1700359.
17. Wang, S.; Copeland, L.; *Crit. Rev. Food Sci. Nutr.* **2015**, *55*, 1081.
18. Han, Z.; Zeng, X. A.; Yu, S. J.; Zhang, B. S.; Chen, X. D.; *Innovative Food Sci. Emerging Technol.* **2009**, *10*, 481.
19. Han, Z.; Zeng, X.-a.; Zhang, B.-s.; Yu, S.; *J. Food Eng.* **2009**, *93*, 318.
20. Giteru, S. G.; Oey, I.; Ali, M. A.; *Trends Food Sci. Technol.* **2018**, *72*, 91.
21. Li, Q.; Wu, Q.-Y.; Jiang, W.; Qian, J.-Y.; Zhang, L.; Wu, M.; Rao, S.-Q.; Wu, C.-S.; *Carbohydr. Polym.* **2019**, *207*, 362.
22. Li, D.; Yang, N.; Jin, Y.; Zhou, Y.; Xie, Z.; Jin, Z.; Xu, X.; *Carbohydr. Polym.* **2016**, *153*, 535.
23. Li, D.; Yang, N.; Zhou, X.; Jin, Y.; Guo, L.; Xie, Z.; Jin, Z.; Xu, X.; *Food Hydrocolloids* **2017**, *71*, 198.
24. Zhu, F.; *Trends Food Sci. Technol.* **2018**, *75*, 158.
25. *OriginPro*, version 9.5; OriginLab Corporation, USA, 2019.
26. Hulleman, S. H. D.; Kalisvaart, M. G.; Janssen, F. H. P.; Feil, H.; Vliegenthart, J. F. G.; *Carbohydr. Polym.* **1999**, *39*, 351.
27. Doutch, J.; Bason, M.; Franceschini, F.; James, K.; Clowes, D.; Gilbert, E. P.; *Carbohydr. Polym.* **2012**, *88*, 1061.
28. Yang, Z.; Swedlund, P.; Hemar, Y.; Mo, G.; Wei, Y.; Li, Z.; Wu, Z.; *Int. J. Biol. Macromol.* **2016**, *85*, 604.
29. Wang, Y.-J.; Truong, V.-D.; Wang, L.; *Carbohydr. Polym.* **2003**, *52*, 327.
30. Utrilla-Coello, R. G.; Hernández-Jaimes, C.; Carrillo-Navas, H.; González, F.; Rodríguez, E.; Bello-Pérez, L. A.; Vernon-Carter, E. J.; Alvarez-Ramirez, J.; *Carbohydr. Polym.* **2014**, *103*, 596.
31. Wang, Y.; Xiong, H.; Wang, Z.; Din, Z.-ud; Chen, L.; *Int. J. Biol. Macromol.* **2017**, *103*, 819.
32. Chen, P.; Yu, L.; Chen, L.; Li, X.; *Starch/Staerke* **2006**, *58*, 611.
33. Buleon, A.; Gallant, D. J.; Bouchet, B.; Mouille, G.; D'Hulst, C.; Kossmann, J.; Ball, S.; *Plant Physiol.* **1997**, *115*, 949.
34. Cheetham, N. W. H.; Tao, L.; *Carbohydr. Polym.* **1998**, *36*, 277.
35. Jenkins, P. J.; Donald, A. M.; *Carbohydr. Res.* **1998**, *308*, 133.
36. Chen, P.; Xie, F.; Zhao, L.; Qiao, Q.; Liu, X.; *Food Hydrocolloids* **2017**, *69*, 359.
37. Jenkins, P. J.; Donald, A. M.; *Starch/Staerke* **1997**, *49*, 262.
38. Wang, S.; Copeland, L.; *Carbohydr. Polym.* **2012**, *87*, 1507.
39. Atichokudomchai, N.; Shobsngob, S.; Varavinit, S.; *Starch/Staerke* **2000**, *52*, 283.
40. Cardoso, M. B.; Westfahl Jr., H.; *Carbohydr. Polym.* **2010**, *81*, 21.
41. Blazek, J.; Gilbert, E. P.; *Carbohydr. Polym.* **2011**, *85*, 281.
42. Porod, G. In *Small-Angle X-Ray Scattering*; Glatter, O.; Kratky, O., eds.; Academic Press: London, UK, 1982, p. 377.

Submitted: February 3, 2019
Published online: July 23, 2019